

**Effects of random motions on critical point measurements:
liquid-gas systems in microgravity**

Mark Cowan and Joseph Rudnick

Department of Physics, UCLA

Los Angeles, California 90024-1547

M. Barinatz

Jet Propulsion Laboratory

California Institute of Technology

Pasadena, California, 91109

(September 14, 1995)

Abstract

The effects of random accelerations on the measurements of quantities in the vicinity of the liquid-gas critical point are considered when the system is in a microgravity environment. These accelerations couple to the order parameter through the transverse component of the velocity field, whose dynamics are also governed by critical point properties of the liquid-gas system. The action of the accelerations is amplified by the singular static and dynamic response of the gas-liquid system. A general formulation, based on “Model II” critical dynamics allows for the calculation of a variety of quantities. It is found that the random accelerations expected in a microgravity environment will not compromise the accuracy of any experiment that is currently envisioned.

Typeset using REVTeX

I. INTRODUCTION

Space-based laboratories present the researcher with an environment in which the properties of some critical point systems of current interest can be investigated with unprecedented accuracy [1]. Among the most important of those systems are liquids having a critical or multicritical point. It has been known for a long time that the variations in the pressure of a liquid sample due to the earth's gravitational action impose the ultimate limit on the accuracy of any measurement of critical point properties in an earthbound laboratory [2]. The effects of gravity are especially pronounced for the very important and widely-studied liquid-gas critical point of a single chemical component, which corresponds to the termination of the co-existence curve separating the liquid and vapor phases [2]. For this system, the order parameter couples directly to the gravitational field. Given the formal correspondences that follow from the universality of critical behavior, the liquid-gas critical point is effectively identical to that of a uniaxial ferromagnet whose Curie-point behavior has been disrupted by the action of a spatially varying, externally-generated magnetic field.

The potential benefits of improved measurements of critical point properties in simple gas-liquid systems are profound. These systems represent the first discovered example of critical point behavior [4]. They are also exemplars of a broad class of systems. The exponents that quantify the critical behavior of simple gas-liquid systems should also apply to analogous behavior in uniaxial ferro- and antiferromagnets at the Curie and Néel points, two-component mixtures at the demixing transition, and the Ising model [5]. This last system is, in itself, extremely important. The mathematical simplicity of the Ising model's Hamiltonian allows for relative ease of renormalization-group-based analysis [6], Monte Carlo simulations [7] and high- and low-temperature expansions [8]. Because of this, the predicted values of the critical exponents of the simple gas-liquid universality class in three dimensions are the most precise and reliable of all non-exact theoretical results in the study of critical phenomena. An accurate experimental determination of the critical properties of a simple gas-liquid system represents a stringent, possibly decisive, experimental test of some of the

most important theoretical models and techniques--as well as some of the most influential ideas about the behavior of interacting systems--that have been developed in the past four decades.

The environment in a space-based laboratory is not entirely free of gravitational effects. There are, of course, the forces due to the gravitational interactions between all the matter on the spacecraft. Much more importantly, random accelerations, which are unavoidable in an orbiting laboratory, give rise to effective gravitational-like forces. Unlike the earth's gravitational field these forces fluctuate in time, but they nevertheless can act to limit the ultimate precision with which critical point measurements can be performed. In this paper, we present the results of a study of the effects of fluctuating linear and rotational accelerations on the static and dynamics of a simple gas-liquid system in the immediate vicinity of its critical point. This study represents the completion of work reported on previously [9]. The approach utilized here is to be contrasted with the calculation of Herrrell [10], who utilized an approximate, self-consistent fluctuation-dissipation relation to obtain predictions for the effects of random linear accelerations on the wave-vector-dependent thermal conductivity. We develop an approach that yields a larger number of results, albeit in the long-wavelength, low-frequency limit.

The results of this theoretical analysis will be applied to the ^3He critical point, which is, now being considered as a model liquid-gas system for study in a space environment [11]. We find that the random motions expected in a microgravity environment will not compromise the accuracy of any foreseeable experiment.

11. PERTURBING FORCES DUE TO RANDOM MOTIONS OF THE APPARATUS

The critical dynamics of a liquid-gas system are controlled by the transverse (i.e. divergence-free) component of the velocity field. An essential stage in the assessment of the effects of small random motions on the critical properties of a liquid-gas system is, thus,

to determine the exact manner in which random linear accelerations and rotations couple to the transverse velocity field. We will find that there are four such couplings, each of which can produce an effect on the critical point properties.

As our first step, however, it is necessary to consider the effect of small fluctuations in the linear velocity of the system on the purely longitudinal (i.e. irrotational) velocity field. If a container suffers only linear accelerations then the most reasonable assumption that one can make is that the fluid contained in it translates with the container as if it were a solid body. However, near its critical point a fluid is highly compressible, and because of that its velocity can vary considerably from point to point. Furthermore, the system has normal modes that can, in principle, be resonantly excited if variations in the container's motion have the proper frequency. Such a resonant excitation of modes could, in principle, lead to a tremendous amplification of the effects of small accelerations. This issue is addressed in the next Section. Resonant excitation of normal modes does not occur in the parameter range of interest in this study. However, because of the nonvanishing compressibility of the liquid-gas system, modes will be nonresonantly excited. The lowest-lying modes will be the most strongly excited by this mechanism.

Linear accelerations *only* couple directly to the longitudinal component of the velocity field. There are two ways in which the purely longitudinal inertial forces induced by linear motion of the container indirectly perturb the transverse component of the velocity field. First, the effective gravitational force can have a transverse component, as the result of fluctuations in the mass density $\rho(\mathbf{x}, t)$. In "fourier space" this component can be written as

$$\mathbf{F}_1(\mathbf{k}, t) = \mathbf{T}(\mathbf{k}) \cdot (\mathbf{a}(t)\rho(\mathbf{k}, t)), \quad (2.1)$$

where $\mathbf{a}(t)$ is the fluctuating linear acceleration of the container, and the projection operator \mathbf{T} , with elements $T'_{ij}(\mathbf{k}) = \delta_{ij} - k_i k_j / k^2$, selects the transverse part of the inertial force $\mathbf{a}(t)\rho(\mathbf{x}, t)$. This is the coupling that gives rise to the perturbations calculated by Ferrell [10]. A second coupling of the linear accelerations to the transverse velocity is via the

convective contribution, $(\mathbf{v} \cdot \nabla)\mathbf{v}$, to the total time derivative of the velocity in its equation of motion (see Eq.(A8c)). We begin by writing

$$(\mathbf{v} \cdot \nabla)\mathbf{v} = \frac{1}{2}\nabla v^2 - \mathbf{v} \times (\nabla \times \mathbf{v}). \quad (2.2)$$

Decomposing the velocity field, \mathbf{v} , into transverse and longitudinal components, \mathbf{v}_t and \mathbf{v}_l , we find that the only contribution to the convective part of the time derivative that has a non-zero transverse component is

$$\mathbf{v}_l \times (\nabla \times \mathbf{v}_t). \quad (2.3)$$

The transverse contribution to the effective force associated with Eq.(2.3) can be extracted in fourier space. It is

$$\mathbf{F}_2(\mathbf{k}, t) = -\mathbf{v}_t(\mathbf{k})(\mathbf{v}_l \cdot \mathbf{k}). \quad (2.4)$$

Implicit in this result is the assumption that the longitudinal component of the velocity field is effectively constant throughout the container.

Random rotations of a container will also give rise to effective forces on the liquid-gas system contained therein. The most important of these are the Coriolis forces. The general form of such forces is

$$\mathbf{F}_C = 2\boldsymbol{\Omega} \times \mathbf{v}. \quad (2.5)$$

in this case there is direct coupling to the transverse component of the velocity field. The transverse component of the Coriolis force given by Eq. (2.5), with $\mathbf{v} = \mathbf{v}_t$ is, in fourier space,

$$\mathbf{F}_3 = 2\boldsymbol{\Omega} \cdot \mathbf{k}(\mathbf{k} \times \mathbf{v}_t)/k^2. \quad (2.6)$$

Finally, the component of the rotational velocity $\boldsymbol{\Omega}$ that is transverse to both $\mathbf{v}_t(\mathbf{k})$ and $\mathbf{v}_l(\mathbf{k})$ -- denoted by $\boldsymbol{\Omega}_\perp$ -- couples the longitudinal and transverse velocity fields. That is, the transverse velocity field responds to an effective force given by

$$\mathbf{F}_{4a} = 2(\boldsymbol{\Omega}_{\perp} \times \mathbf{v}_t), \quad (2.7)$$

while the longitudinal velocity field is subject to the effective force

$$\mathbf{F}_{4b} = 2(\boldsymbol{\Omega}_{\perp} \times \mathbf{v}_t). \quad (2.8)$$

Note that the force \mathbf{F}_1 can be thought of as ‘(direct’, in that it does not depend directly on the velocity fields. By contrast, the forces \mathbf{F}_2 , \mathbf{F}_3 , and $\mathbf{F}_{4a,4b}$ which have a linear dependence on \mathbf{v} , are ‘parametric’ in form.

As it turns out, the force \mathbf{F}_1 , which is central to Ferrell’s calculations, does not play a role in our approach.

111. MOTION OF FLUID IN A VIBRATING CONTAINER

The next step in the assessment of the effects of random motions of a container is to determine the response of the fluid to those motions. To simplify the discussion of the effects of linear accelerations, we assume a one-dimensional geometry. The linearized hydrodynamical equations that control the evolution of the velocity field $v(x, t)$ and the mass density $\rho(x, t)$ are

$$\rho_0 \frac{\partial v}{\partial t} = -[\rho_0 \beta_s]^{-1} \frac{\partial \rho}{\partial x} + \bar{\eta} \frac{\partial^2 v}{\partial x^2}, \quad (3.1)$$

$$\frac{\partial \rho}{\partial t} = -\rho_0 \frac{\partial v}{\partial x}, \quad (3.2)$$

where ρ_c is the equilibrium fluid density, taken to be the critical density, β_s is the isentropic compressibility and $\bar{\eta}$ is the viscosity. In terms of the shear viscosity, η_1 , and the bulk viscosity, η_2 , $\bar{\eta} = \eta_1/3 + \eta_2$.

If we write

$$v(x, y) = v_0 e^{i(kx - \omega t)}, \quad (3.3a)$$

$$\rho(x, y) = \Delta \rho e^{i(kx - \omega t)}, \quad (3.3b)$$

then Eqs. (3.1) and (3.2) become

$$-i\omega v_0 \rho_0 = \frac{ik\Delta\rho}{\rho_0\beta_s} - k^2\bar{\eta}v_0, \quad (3.4)$$

$$i\omega\Delta\rho = ik\rho_0v_0. \quad (3.5)$$

These two equations imply the following dispersion relation:

$$\omega^2 - \frac{k^2}{\rho_0\beta_s} - \frac{i\omega k^2\bar{\eta}}{\rho_0} = 0. \quad (3.6)$$

Solving for the wave vector k :

$$\begin{aligned} k &= \sqrt{\frac{\rho_0\beta_s\omega^2}{1 - i\omega\beta_s\bar{\eta}}} \\ &= \sqrt{\frac{(\omega/c)^2}{1 - i\omega\tau}} \\ &\equiv k_R + ik_I. \end{aligned} \quad (3.7)$$

in the equation above $\tau = \beta_s\bar{\eta}$ is the relaxation time and the undamped sound velocity c is given by

$$c = 1/\sqrt{\rho_0\beta_s}. \quad (3.8)$$

Suppose, now, that we are interested in the behavior of the velocity field inside a steadily vibrating container. The most general solution to the one-dimensional equations of motion - the time-dependence being sinusoidal with angular frequency ω - is

$$v(x, t) = \left[A e^{ik_R x - k_I x} + B e^{-ik_R x + k_I x} \right] e^{-i\omega t} + \left[C e^{-ik_R x - k_I x} + D e^{ik_R x + k_I x} \right] e^{i\omega t}. \quad (3.9)$$

If we impose the following boundary conditions on the velocity field at the ends of the container, at $x = \pm L$,

$$v(L, t) = v(-L, t) = V \cos \omega t, \quad (3.10)$$

then the coefficients in Eq. (3.9) must take on the following values

$$A = B = \frac{V}{4 \cos(k_R L + ik_I L)}, \quad (3.11a)$$

$$C = D = \frac{V}{4 \cos(k_R L - ik_I L)}. \quad (3.11b)$$

The velocity field inside the container ($-L \leq x \leq L$) is

$$v(x, t) = V \Re \left[e^{-i\omega t} \frac{\cos(k_R x + i k_I x)}{\cos(k_R L + i k_I L)} \right]. \quad (3.12)$$

The denominator in Eq. (3.12) has a resonant form in the vicinity of $\cos k_R L = 0$, or $k_R = (n + 1/2)\pi/L$. To explore the resonant response in greater detail, we evaluate the integrated weight of $v(x, t)$:

$$\begin{aligned} \int_{-L}^L v(x, t) dx &= V \Re \int_{-L}^L \cos(k_R x + i k_I x) dx \frac{e^{-i\omega t}}{\cos(k_R L + i k_I L)} \\ &= 2V \Re \left[\frac{e^{-i\omega t}}{k_R + i k_I} \tan(k_R L + i k_I L) \right] \\ &= 2V \Re \left[\frac{e^{-i\omega t}}{k_R + i k_I} \frac{\sin k_R L \cos k_R L + i \sinh k_I L \cosh k_I L}{\cos^2 k_R L + \sinh^2 k_I L} \right]. \end{aligned} \quad (3.13)$$

If $\omega\tau \ll 1$ in the vicinity of the resonance, then the amplitude of the velocity goes as

$$\frac{\omega^2 \tau L / c}{\left((\omega L / c - (n + 1/2)\pi)^2 + (\omega^2 \tau L / c)^2 \right)}. \quad (3.14)$$

Now, the linear dimension of a container in a the kind of low-temperature experiment likely to be performed in a microgravity environment is ≈ 10 cm. The wavevector k_R of the lowest-lying resonant mode is, then, given by $k_R \approx 2\pi/20 \text{ cm} \approx 0.33 \text{ cm}^{-1}$. In the case of near-critical ^3He , sound in the relevant frequency range propagates adiabatically, and its speed is equal to $3.2 \times 10^4 t^{0.057} \text{ Hz}$, where t is the reduced temperature [$t = (T - T_{\text{critical}})/T_{\text{critical}}$] (see table 111). The frequency, ω , of this mode is, thus, equal to $\sim 1 \times 10^4 t^{0.057} \text{ Hz}$. If $t = 10^{-7}$, then $\omega = 4 \times 10^3 \text{ Hz}$. The width of the resonance at this frequency is equal to $Q = \omega\tau/2 = f/\Delta f$ with $\tau = 3.8 \times 10^{-12} t^{-0.14} \text{ sec}$. At $t = 10^{-7}$, $\omega\tau \approx 2 \times 10^{-7}$, so the mode is very well-defined. As the characteristic frequencies of random linear velocities in a space environment are expected to be in the tens of Hertz [12], resonant excitation of acoustic modes must be considered unlikely.

The frequency at which the container is vibrating in a space environment is small compared to the frequency of the lowest-lying mode, and we can expand the expression in Eq. (3.12) with respect to k_R . The velocity is given by

$$v(x, t) \approx V e^{-i\omega t} \left[1 - \frac{1}{2} k_R^2 (x^2 - L^2) \right]. \quad (3.15)$$

In the frame of reference of the vibrating container,

$$v(x, t) \rightarrow V e^{-i\omega t} \frac{1}{2} k_r^2 (L^2 - x^2). \quad (3.16)$$

In the center of the container ($x = 0$) the velocity has a magnitude equal to $V(1 + \frac{1}{2} k_R L^2)$, so the velocity of the fluid in the reference frame of the container is $V k_R^2 L^2 = V(\omega L / C_S)^2$.

The quantity C_S is the adiabatic speed of sound, as given above.

The above results allow us to check immediately for the density fluctuations induced by vibrations in the container and the rate at which heat is generated as the result of viscous damping of the fluid's motion.

The small fluctuations in density associated with the velocity variation above are given by Eqs. (3.2) and (3.16):

$$\delta\rho(x, \omega) = i\rho_c \frac{\omega x v}{C_s^2}. \quad (3.17)$$

The mean square variation in the density is

$$\delta\rho(x, \omega) \delta\rho(x, -\omega) = \rho_c^2 \frac{\omega^2 x^2 V^2}{C_s^4}. \quad (3.18)$$

Averaging over an ensemble of random velocities:

$$\langle \delta\rho(x, \omega) \delta\rho(x, -\omega) \rangle = \frac{\rho_c^2 \omega^2 x^2 \langle v(\omega) v(-\omega) \rangle}{C_s^4}. \quad (3.19)$$

In the above Equation, $\langle \delta\rho(x, \omega) \delta\rho(x, -\omega) \rangle$ is the spectral density of mass density fluctuations and $\langle v(\omega) v(-\omega) \rangle$ is the spectral density of random container velocities. Using $\langle a(\omega) a(-\omega) \rangle = \omega^2 \langle v(\omega) v(-\omega) \rangle$, where $\langle a(\omega) a(-\omega) \rangle$ is the spectral density of accelerations, we end up with

$$\langle \delta\rho(x, \omega) \delta\rho(x, -\omega) \rangle = \frac{\rho_c^2 x^2}{C_s^4} \langle a(\omega) a(-\omega) \rangle. \quad (3.20)$$

The root mean square of density fluctuations is, then,

$$\frac{\rho_c x}{C_s^2} \sqrt{\int \langle a(\omega) a(-\omega) \rangle d\omega} \leq \frac{\rho_c L}{C_s^2} \sqrt{\int \langle a(\omega) a(-\omega) \rangle d\omega}. \quad (3.21)$$

Thus, the fractional variation in density due to random accelerations of the container is $\approx \frac{L}{C_s^2} \sqrt{\int \langle a(\omega) a(-\omega) \rangle d\omega}$. We can also utilize the results for the velocity in a vibrating container to estimate the rate at which the temperature will rise as a result of viscous damping of the induced velocity fluctuations: the end result is

$$\frac{dT}{dt} \approx \frac{L^2 \bar{\eta}}{C_s^4 \rho_c c_P} \int \omega^2 \langle a(\omega) a(-\omega) \rangle d\omega. \quad (3.22)$$

IV. RANDOM LINEAR ACCELERATIONS AND TRANSPORT COEFFICIENTS

Because of the coupling of longitudinal velocity fluctuations to the transverse velocity through the convective contribution to the total hydrodynamic time derivative, (see Eq. (2.4)), random vibrations of the container will alter transport coefficients, most notably the thermal conductivity, κ and the shear viscosity η_1 . The changes in the transport coefficients due to mode-coupling can be calculated with the use of a modification of the standard perturbation-theoretical formalism. The diagrammatic notation is summarized in Fig. 1. It is an adaptation of the approach appropriate to critical dynamics in which there is a single fluctuating field, characteristically the energy density. The order parameter propagator in the case at hand is more complicated, as we must take into account fluctuations in both the energy density and the mass density. The scalar order parameter is a combination of those two fields. The underlying dynamics are outlined in Appendix A. The order parameter propagator is obtained by inverting the response equations

$$c_1(k, \omega) [-i\omega + \frac{\kappa k^2}{\rho_c^2} a(k)] + \rho_1(k, \omega) \frac{\kappa k^2}{\rho_c^2} b(k) = f_c \quad (4.1a)$$

$$c_1(k, \omega) \frac{ik^2 b(k) \rho_c}{\omega} + \rho_1(k, \omega) [-i\omega + \frac{2ik^2 c(k) \rho_c}{\omega} + \frac{\bar{\eta} k^2}{\rho_c}] = f_\rho. \quad (4.1b)$$

The solution is

$$\begin{aligned}
\begin{pmatrix} \epsilon_1(k, \omega) \\ \rho_1(k, \omega) \end{pmatrix} &= \frac{1}{D(k, \omega)} \begin{pmatrix} -i\omega + \frac{2ik^2 c(k) \rho_c}{\omega} + \frac{\bar{\eta} k^2}{\rho_c} & -\frac{\kappa k^2 b(k)}{\rho_c^2} \\ -\frac{ik^2 b(k) \rho_c}{\omega} & -i\omega + \frac{\kappa k^2}{\rho_c^2} 2a(k) \end{pmatrix} \begin{pmatrix} f_\epsilon \\ f_\rho \end{pmatrix} \\
&\equiv \begin{pmatrix} g_{\epsilon\epsilon}(k, \omega) & g_{\epsilon\rho}(k, \omega) \\ g_{\rho\epsilon}(k, \omega) & g_{\rho\rho}(k, \omega) \end{pmatrix} \begin{pmatrix} f_\epsilon \\ f_\rho \end{pmatrix}.
\end{aligned} \tag{4.2}$$

The g 's in Eq. (4.2) are the components of the order parameter propagator, and the function $D(k, \omega)$ is given by

$$D(k, \omega) = \begin{vmatrix} -i\omega - \frac{2ik^2 c(k) \rho_c}{\omega} + \frac{\bar{\eta} k^2}{\rho_c} & -\frac{\kappa k^2 b(k)}{\rho_c^2} \\ -\frac{ik^2 b(k) \rho_c}{\omega} & -i\omega + \frac{2\kappa k^2 a(k)}{\rho_c^2} \end{vmatrix} = \frac{i\kappa k^4 b(k)^2}{\omega \rho_c} \tag{4.3}$$

By contrast, the transverse velocity propagator $G_T(k, \omega)$ has the standard form

$$G_T(k, \omega) = \frac{1}{-i\omega + \eta_1 k^2 / \rho_c}. \tag{4.4}$$

All quantities in the above equations are defined in Appendices A, B and C.

The coupling of vibration-induced fluctuations in the longitudinal velocity to the transverse velocity leads to the following insertion on the transverse velocity propagator line [13,14]

$$\begin{aligned}
\Delta\Sigma(k, \omega) &= \int d\omega' k_{\parallel}^2 \langle v(\omega') v(-\omega') \rangle G_T(k, \omega + \omega') \\
&= \int d\omega' \frac{k_{\parallel}^2}{-2i(\omega + \omega') + \eta_1 k^2 / \rho_c} \langle v(\omega') v(-\omega') \rangle.
\end{aligned} \tag{4.5}$$

This insertion is illustrated in Fig. 1. The quantity k_{\parallel} is the component of the wave vector k that is parallel to the longitudinal velocity fluctuations. The one-loop correction to the thermal conductivity is of the form shown in Fig. 2. After some reduction, one finds for the leading order contribution to the thermal conductivity

$$\frac{2}{3} k_B T \rho_c \int \frac{d^3 p}{(2\pi)^3} \frac{1}{a'(p) (-i\omega + \eta_1 p^2 / \rho_c + \Delta\Sigma(p, 0))}, \tag{4.6}$$

where $a'(k) = a(k) - b(k)^2 / 4a(k)c(k)$ is the static energy density susceptibility. Furthermore, as discussed in Appendix B, $a(0) \propto c_p^{-1}$. Utilizing an Ornstein-Zernicke-type form for $a'(k)$ ($a'(k) = \xi^2 + k^2$) and carrying out the integrations over the wave vector p , we arrive at

the following correction to the thermal diffusivity to lowest nontrivial order in the random linear motions

$$\delta D_T = \frac{1}{9\pi} \frac{k_B T'}{\rho_c} \left(\frac{\rho_c}{\eta_1} \right)^3 \int d\omega' \langle a(\omega') a(-\omega') \rangle \frac{\omega'^2 L^4}{C_s^4} \frac{1}{1 + \frac{i\omega' \rho_c \xi^2}{\eta_1} \sqrt{-i\omega' \rho_c / \eta_1}} - \xi \Bigg|, \quad (4.7)$$

where the thermal diffusivity is given by

$$D_T = \frac{K}{T_c c_P \rho_c}, \quad (4.8)$$

and the quantities in Eq. (4.8) are defined in §able I.

The renormalization of the transverse velocity propagator also leads—quite directly—to results for the alteration of the effective shear viscosity. The fractional change in η_1 follows from consideration of the insertion $\Delta\Sigma(k, \omega)$. Setting $\omega = 0$, we find

$$\begin{aligned} \Delta\Sigma(k, 0) &\rightarrow \frac{1}{3} k^2 \int d\omega' \frac{\langle a(\omega') a(-\omega') \rangle \omega'^2 L^4}{\eta_1 k^2 / \rho_c - i\omega' C_s^4} \\ &= \frac{1}{3} k^2 \int \frac{\langle a(\omega') a(-\omega') \rangle \eta_1}{(\eta_1 k^2 / \rho_c)^2 + \omega'^2} \frac{k' \omega'^2 L^4}{\rho_c C_s^4} \end{aligned} \quad (4.9)$$

Taking the limit $k \rightarrow 0$, we see that $\Delta\Sigma \propto k^4$, which means that random linear accelerations of the container lead to *no* change in the effective shear viscosity.

V. EFFECTS OF RANDOM ROTATIONS ON TRANSPORT COEFFICIENTS AND THERMODYNAMIC FUNCTIONS

We will consider separately the two forcing terms established in Section II:

A. Rotations that couple the transverse velocity field to itself

The insertion on the transverse propagator line associated with the force \mathbf{F}_{4a} is illustrated in Fig. 1. It leads immediately to the insertion on the transverse velocity propagator line shown in Fig. 3. This insertion has the form

$$\begin{aligned}\Delta\Sigma(k, \omega) &= - \int d\omega' \frac{\langle \Omega_{||}(\omega) \Omega_{||}(-\omega) \rangle}{-i(\omega + \omega') + \eta_1 k^2 / \rho_c} \frac{\eta_1 k^2}{\rho_c} \int d\omega' \frac{\langle \Omega_{||}(\omega) \Omega_{||}(-\omega) \rangle}{(\omega + \omega')^2 + (\eta_1 k^2 / \rho_c)^2} \\ &\rightarrow \frac{\eta_1 k^2}{\rho_c} \int d\omega' \frac{\langle \Omega_{||}(\omega') \Omega_{||}(-\omega') \rangle}{\omega'^2},\end{aligned}\quad (5.1)$$

The quantity $\Omega_{||}$ is the component of the rotation vector $\vec{\Omega}$ parallel to the longitudinal velocity field. The final limit above is at $w = 0$ and as $k \rightarrow 0$. We have, as the fractional change in the shear viscosity,

$$\int d\omega \frac{\langle \Omega_{||}(\omega) \Omega_{||}(-\omega) \rangle}{\omega^2} \quad (5.2)$$

In the equations above $\langle \Omega_{||}(\omega) \Omega_{||}(-\omega) \rangle$ is the spectral density of random rotations.

Because of the way in which the one-loop correction to the thermal conductivity depends on the shear viscosity (see Eq. (4.4) and Ref. [14J], the fractional change in κ or D_T is the same as the fractional shift in η_1 . Note that both shifts are independent of temperature and other parameters.

B. Rotations that couple the transverse and longitudinal velocity fields

The insertion on the transverse propagator is as illustrated in Fig. 1. Using Eq. (4.2) and the relationship (A1) between the mass density and the longitudinal velocity field, we have for the alteration of the transverse velocity field propagator

$$\begin{aligned}& - \int d\omega' \langle \Omega_{\perp}(\omega') \Omega_{\perp}(-\omega') \rangle \\ & \frac{-i(\omega + \omega') + 2\kappa k^2 a(k) / \rho_c^2}{(-i(\omega + \omega') + k^2 (2ic(k) \rho_c / (\omega + \omega') + \bar{\eta} / \rho_c)) (-i(\omega + \omega') + 2a(k) \kappa^2 / \rho_c^2) - i\kappa k^4 b(k)^2 / (\omega + \omega') \rho_c} \\ & \rightarrow \frac{\bar{\eta}}{\rho_c} \int d\omega' \frac{\langle \Omega_{\perp}(\omega') \Omega_{\perp}(-\omega') \rangle}{\omega'^2}\end{aligned}\quad (5.3)$$

Because of the coupling between the two velocity fields, the change in the shear viscosity is now proportional to the viscosity appropriate to the longitudinal velocity field.

The alteration above in the shear viscosity yields, as in the previous Subsection, a perturbation in the thermal conductivity that is proportional to $(\bar{\eta} / \rho_c) \int d\omega' (\langle \Omega_{\perp}(\omega') \Omega_{\perp}(-\omega') \rangle / \omega'^2)$.

Finally, there is an insertion in the propagator $g_{\epsilon\epsilon}(k, \omega)$ analogous to the transverse velocity insertion illustrated in Fig. 3. This insertion has the following first order effect on the propagator

$$\int d\omega' g_{\epsilon\rho}(k, \omega) G_T(k, \omega + \omega') g_{\rho\epsilon} \langle \Omega_{\perp}(\omega') \Omega_{\perp}(-\omega') \rangle. \quad (5.4)$$

After some reduction, we find for the effective insertion

$$\frac{b(0)^2 \kappa}{4c(0)^2 \rho_c^3} \int d\omega' \langle \Omega_{\perp}(\omega') \Omega_{\perp}(-\omega') \rangle, \quad (5.5)$$

the above being valid in the limit of small (k, ω) . This insertion does *not* have the form of a thermal conductivity, in that it does not vanish as k^2 in the limit of long wavelength.

The final contribution above to transport coefficients also produces an alteration in thermodynamic susceptibilities. This is because of the relationship between the dynamical and thermodynamical response inherent in the system of equations discussed in Appendix A:

$$c_P = \lim_{k, \omega \rightarrow 0} \frac{\kappa}{\rho_c^2} g_{\epsilon\epsilon}(k, \omega). \quad (5.6)$$

The fractional shift in c_P is

$$\lim_{k \rightarrow 0} \frac{1}{k^2} \frac{a(k)b(k)^2}{8(a(k) - b(k)^2/(4a(k)c(k)))c(k)\rho_c} \int d\omega' \langle \Omega_{\perp}(\omega') \Omega_{\perp}(-\omega') \rangle. \quad (5.7)$$

The limit $k \rightarrow 0$ is catastrophic because of the first term in (5.7). The combination in the middle approaches ratio $c_P/(c_V C_s^2)$ in that limit, and the integral over the spectrum of random rotations is, of course independent of k . For a bounded system, in which there is a natural lower limit to k , a finite correction to c_P results from (5.7).

There is no change in the specific heat of the system associated with the contributions to κ_T arising from one-loop corrections to that quantity as calculated in previous Sections because cancelling vertex corrections are also generated.

VI. EFFECTS OF RANDOM MOTIONS ON A ^3He CRITICAL POINT EXPERIMENT

As an application of the results derived in the previous Sections, we will calculate the effects of random linear and rotational motion on the properties of ^3He in the vicinity of its liquid-gas critical point. This is with an eye to establishing the limits placed on microgravity critical point measurements by vibrations in an orbiting laboratory. Information on the thermodynamic functions and transport properties in the vicinity of the ^3He critical point is incomplete. There is, in addition, some variability in the data on linear acceleration in a space-based laboratory, and no measurements have been made of rotations in that environment. Because of all this, the calculations reported in this Section will necessarily involve approximations, and results will be accurate as order-of-magnitude estimates at best. Nevertheless, we find that the effects of random, linear accelerations are negligible in any foreseeable critical point experiment. In the case of rotations, sufficient uncertainty exists that one cannot rule them out as a perturbing effect, in the absence of an experimental determination of their magnitude.

A. Linear accelerations

First, we will estimate the density fluctuations and the temperature drift, using the results obtained in Section III. Using Eq. (3.21) and values in Table III we find

$$\frac{\sqrt{\delta\rho^2}}{\rho_c} = 9.77 \times 10^{-9} \frac{\text{sec}^2}{\text{cm}} \sqrt{\int \langle a(\omega) a(-\omega) \rangle d\omega} \times t^{-\alpha}. \quad (6.1)$$

The exponent α in Eq. (6.1) is equal to 0.11, so the temperature dependence of the left hand side is not particularly strong. We have assumed a container with a linear dimension $L \approx 10$ cm. Data from experiments already performed on shuttle vibrations indicate that the largest sources of "g-jitter" give rise to accelerations of order 1 cm/sec^2 with characteristic frequencies of the order of 10 Hz [12]. All this indicates that variations in the density will be no more than a part in 10^8 down to reduced temperatures of 10-8.

Next, we calculate the thermal drift due to viscous damping of the vibration-induced motion of the fluid. Inserting results from Table III (we have utilized the amplitude of C_v as an estimate of the amplitude of c_P) we find

$$\frac{dT}{dt} \approx 1.5 \times 10^{-27} \frac{^\circ\text{K}}{\text{sec}} t^{\nu(2-\eta-x_\nu)-2\alpha} \int \omega^2 \langle a(\omega) a(-\omega) \rangle d\omega. \quad (6.2)$$

This effect is absolutely negligible.

Finally, Eq. (4.7) allows us to see what effect random line.m motion has on the thermal diffusivity. At very low reduced temperatures the correlation length ξ dominates all other lengths in the integral and we find

$$\begin{aligned} \frac{\delta D_T}{D_T} &= \frac{1}{9\pi} \frac{k_B T}{\rho_c D_T} \frac{L^4}{C_s^4 \eta_1} \left(\frac{\rho_c}{C_s \eta_1} \right)^3 \xi \int \omega^2 \langle a(\omega) a(-\omega) \rangle d\omega \\ &= 7.56 \times 10^{-24} t^{-\nu(3-\eta-x_\lambda)-2\alpha+3x_\eta} \int \omega^2 \langle a(\omega) a(-\omega) \rangle d\omega. \end{aligned} \quad (6.3)$$

The power of the reduced temperature is ≈ -1.5 . At no experimentally achievable value of t will the above effect be of any importance.

B. Rotations

Here one is hampered by lack of information concerning the random rotations on the spacecraft. However, it is possible to come up with a very rough estimate of the spectral density, $\langle \Omega(\omega) \Omega(-\omega) \rangle$. If we assume $\Omega(\omega) \approx v(\omega)/L_s$, where L_s is the size of the shuttle, which we take to be ≈ 10 m, then the effects of $\Omega_{||}$ of transport properties, as given by Eq. (5.2), are

$$\int d\omega \frac{\langle a(\omega) a(-\omega) \rangle}{\omega^4 L_s^2} \quad (6.4)$$

If we replace w in the integrand above by 10 Hz and the integrated spectral density of accelerations by $1 \text{ cm}^2/\text{sec}^4$ we arrive at a fractional effect of $\Omega_{||}$ of a part in 10^{10} . However this estimate is extremely crude, and there may be errors of a few orders of magnitude. The same estimate applies for the effect of Ω_{\perp} on the shear viscosity- assuming that η_1 and $\bar{\eta}$ are close in magnitude.

As for the consequences on the thermal response of Ω_{\perp} , we find for the fractional change in both D_T and C_p

$$\begin{aligned} \frac{\delta D_T}{D_T} - \frac{\delta C_p}{C_p} &= \frac{c_P L^2}{c_V C_s^2} \int d\omega \langle \Omega_{\perp}(\omega) \Omega_{\perp}(-\omega) \rangle \\ &\approx 10^{-7} \text{sec}^2 t^{-\nu(2-\eta)} \int d\omega \langle \Omega_{\perp}(\omega) \Omega_{\perp}(-\omega) \rangle. \end{aligned} \quad (6.5)$$

The quantity L in Eq. (6.5) is the size of the container of ^3He , which we take to be 10 cm. Once again, to within the very large errors resulting from our uncertainties regarding the spectrum of rotations, we find that there is no observable effect at an achievable reduced temperature of $t = 10^{-8}$.

VII. CONCLUSIONS

We have developed expressions defining the effects of fluctuating linear and rotational accelerations on static and dynamic phenomena near a liquid-gas critical point. These expressions are valid in the long-wavelength, low-frequency limit. The results of this analysis were applied to the properties of ^3He in the vicinity of its critical point. Using g-jitter data from previous space shuttle flights, we find that random linear motions expected in future microgravity experiments should not affect measurements of critical point phenomena to reduced temperatures of 10^{-8} . At this time, measurements of random rotational motions in the space shuttle are not available. However, using estimates for the spectrum of random rotations we also find that there will be negligible effects on critical point phenomena.

ACKNOWLEDGEMENTS

The research described in this article was carried out by the Jet Propulsion Laboratory, California Institute of Technology, under contract with the National Aeronautics and Space Administration.

APPENDIX A: HYDRODYNAMICS OF A SIMPLE LIQUID-GAS SYSTEM NEAR THE CRITICAL POINT

The dynamics of a simple liquid-gas system consists of the following three equations:

- Conservation of mass, which relates the mass density, $\rho(\mathbf{x}, t)$ to the mass current, $\mathbf{j}(\mathbf{x}, t) = \rho(\mathbf{x}, t)\mathbf{v}(\mathbf{x}, t)$

$$\frac{\partial \rho}{\partial t} + \nabla \cdot \mathbf{j} = 0. \quad (\text{A1})$$

- Conservation of (thermal) energy—under the processes of convective transport and thermal diffusion

$$\frac{\partial q}{\partial t} + \nabla \cdot \left(\frac{q\mathbf{j}}{\rho} \right) = \kappa \nabla^2 \frac{\delta F}{\delta q} + \Theta(\mathbf{x}, t). \quad (\text{A2})$$

The expression $\delta F / \delta q$ on the right hand side of Eq. (A2) is the functional derivative of the total Helmholtz free energy of the system, F , with respect to $q(\mathbf{x}, t)$, the thermal energy per unit volume. The transport coefficient κ is the thermal conductivity. The last term on the right hand side represents the rapidly-varying contributions to thermal transport that give rise to fluctuations in the energy density. These terms, which have a “white noise” spectrum, satisfy the following version of the fluctuation-dissipation relation in real space:

$$\langle \Theta(\mathbf{x}, t) \Theta(\mathbf{x}', t') \rangle = 2k_B T \kappa \nabla^2 \delta(\mathbf{x} - \mathbf{x}') \delta(t - t'), \quad (\text{A3})$$

or, in wavevector/frequency space,

$$\langle \Theta(\mathbf{k}, \omega) \Theta(\mathbf{k}', \omega') \rangle = 2k_B T \kappa k^2 \delta(\mathbf{k} + \mathbf{k}') \delta(\omega + \omega'). \quad (\text{A4})$$

Equation (A3), or (A4), helps insure the invariance of the Boltzmann distribution $\exp(-F/k_B T)$ under the action of the system’s dynamics.

- Finally, there is the equation expressing the conservation of momentum in the hydrodynamical system:

$$\frac{\partial \mathbf{j}}{\partial t} + \frac{\partial}{\partial x_i} (j v_i) + q(\mathbf{x}, t) \nabla \frac{\delta F}{\delta q(\mathbf{x}, t)} + \rho(\mathbf{x}, t) \nabla \frac{\delta F}{\delta \rho(\mathbf{x}, t)} = \nabla \cdot \vec{\sigma} + \xi(\mathbf{x}, t). \quad (\text{A5})$$

The **first** term on the right hand side of Eq. (A5) is the viscous damping force. In more detail,

$$\begin{aligned} (\nabla \cdot \vec{\sigma})_k &\equiv \frac{\partial}{\partial x_i} \sigma_{ki} \\ &= \eta_1 \nabla^2 v_k + \left[\frac{1}{3} \eta_1 + \eta_2 \right] \frac{\partial}{\partial x_k} \nabla \cdot \mathbf{v}. \end{aligned} \quad (\text{A6})$$

The coefficients η_1 and η_2 are, respectively, the shear and bulk viscosities. The final term on the right hand side of the equation represents the fluctuating forces that act on the velocity field. These forces satisfy the fluctuation-dissipation relation

$$\langle \xi_i(\mathbf{k}, \omega) \xi_j(\mathbf{k}', \omega') \rangle = \left(2k_B T \eta_1 k^2 \delta_{ij} + 2k_B T \left[\frac{1}{3} \eta_1 + \eta_2 \right] k_i k_j \right) \delta(\mathbf{k} + \mathbf{k}') \delta(\omega + \omega'), \quad (\text{A7})$$

which, again helps ensure that the dynamics leave the Boltzmann distribution invariant.

The conservative contributions to the equations of mass, energy and momentum conservation—contained on the left hand sides of Eqs. (A1), (A2) and (A5)—also preserve the Boltzmann distribution, by leaving the total free energy invariant. These equations thus form a dynamical system which encompasses both the macroscopic hydrodynamics of the liquid-gas system and the coarse-grained, thermally-driven fluctuations associated with the microscopic exploration of phase space mandated by the ergodic hypothesis.

Although the parameter set $\rho(\mathbf{x}, t)$, $\mathbf{j}(\mathbf{x}, t)$ and $q(\mathbf{x}, t)$ is the most natural basis for the derivation of equations that satisfy all the conservation laws and invariance principles, further development of the dynamics, especially as they apply in the immediate vicinity of the critical point, is greatly simplified by replacing thermal energy density and mass current by thermal energy per unit mass, $\epsilon(\mathbf{x}, t) = q(\mathbf{x}, t)/\rho(\mathbf{x}, t)$ and the velocity field, $\mathbf{v}(\mathbf{x}, t)$. In terms of the new variable set the equations for mass, energy and momentum conservation are as follows:

$$\frac{\partial \rho}{\partial t} + \nabla \cdot (\rho \mathbf{v}) = 0 \quad (\text{A8a})$$

$$\frac{\partial \epsilon}{\partial t} + \mathbf{v} \cdot \nabla \epsilon = \frac{1}{\rho} \nabla^2 \frac{1}{\rho} \frac{\delta F}{\delta \epsilon} - \frac{1}{\rho} \Theta \quad (\text{A8b})$$

$$\frac{\partial \mathbf{v}}{\partial t} + (\mathbf{v} \cdot \nabla) \mathbf{v} + \frac{1}{\rho} \rho \nabla \frac{\delta F}{\delta \rho} - \frac{\delta F}{\delta \epsilon} \nabla \epsilon = \frac{1}{\rho} \nabla \cdot \vec{\sigma} + \frac{1}{\rho} \xi. \quad (\text{A8c})$$

This set of equations can be thought of as “model H” critical dynamics [13,14], extended to include non-critical dynamical behavior of the longitudinal component of the velocity field.

Now, if the total free energy can be written

$$F = \int f(\rho(\mathbf{x}), \epsilon(\mathbf{x})) d^d x, \quad (\text{A9})$$

where $f(\rho(\mathbf{x}), \epsilon(\mathbf{x}))$ is a purely local function of the mass density and energy per unit mass, then the terms proportional to the derivatives of the free energy on the right hand side of Eq. (A8c) can be re-arranged as follows:

$$\begin{aligned} \rho \nabla \frac{\delta F}{\delta \rho} - \frac{\delta F}{\delta \epsilon} \nabla \epsilon &= \rho \nabla \frac{\partial f}{\partial \rho} \frac{\partial f}{\partial \epsilon} \nabla \epsilon \\ &= \mathbf{v} \left(\rho \frac{\partial f}{\partial \rho} - f(\rho, \epsilon) \right) \cdot \nabla f - \frac{\partial f}{\partial \rho} \nabla \rho - \frac{\partial f}{\partial \epsilon} \nabla \epsilon \\ &= \mathbf{v} \left(\rho \frac{\partial f}{\partial \rho} - f(\rho, \epsilon) \right). \end{aligned} \quad (\text{A10})$$

A straightforward set of thermodynamic arguments leads to the relationship

$$\rho \frac{\partial f}{\partial \rho} - f(\rho, \epsilon) = P(\rho, \epsilon), \quad (\text{A11})$$

with $P(\rho, \epsilon)$ the local pressure. ~bus, if the free energy density is purely local, then the macroscopic driving term in the momentum conservation equation is the gradient of the pressure. In fact, nonlocal contributions to the free energy density, in the form of terms containing spatial derivatives, play an important role in coupling the heat- and mass-transport equations.

APPENDIX B: LINEARIZED HYDRODYNAMICS AND TIME SCALES

Linearized hydrodynamics describe the long wavelength-low frequency behavior of a system close to equilibrium. As the equilibrium state is one in which the free energy is mini-

mized, we write

$$\begin{aligned}
F &= F(\rho_0, \epsilon_0) \\
&+ \int [a(k)\epsilon_1(\mathbf{k}, \omega)\epsilon_1(-\mathbf{k}, -\omega) + b(k)\epsilon_1(\mathbf{k}, \omega)\rho_1(-\mathbf{k}, -\omega) + c(k)\rho_1(\mathbf{k}, \omega)\rho_1(-\mathbf{k}, -\omega)] d^d k \\
&+ O((\rho_1, \epsilon_1)^3).
\end{aligned} \tag{B1}$$

The quantities ρ_1 and ϵ_1 stand for the differences between the mass density and energy per unit volume and the equilibrium values of those quantities. If the free energy density were purely local, then the coefficients $a(k)$, $b(k)$ and $c(k)$ would not vary with the wavevector, \mathbf{k} . Thermodynamics and dimensional considerations mandate the following relationships between the coefficients $a(0)$, $b(0)$, $c(0)$ and standard thermodynamic quantities:

$$a(0) = \frac{\rho_c}{2T_c c_V} \tag{B2a}$$

$$b(0) = \frac{V \left(\frac{\partial T}{\partial V} \right)_S}{T} \tag{B2b}$$

$$c(0) = \frac{1}{2\beta_S \rho_c^2}. \tag{B2c}$$

The quantity c_V is the specific heat at constant volume, and β_S is the adiabatic compressibility. Standard thermodynamic formulas yield the following relationships:

$$a(0) \left(1 - b(0)^2 / 4a(0)c(0) \right) = \frac{\rho_c}{2T_c c_P} \tag{B3a}$$

$$c(0) \left(1 - b(0)^2 / 4a(0)c(0) \right) = \frac{1}{2\beta_T \rho_c^2}, \tag{B3b}$$

where, c_P is the specific heat at constant pressure and β_T is the isothermal compressibility. For a complete list of the thermodynamic functions used in this paper see Table I.

Expanding Eqs.(A8) to first order in v , ρ_1 and ϵ_1 we obtain, in the wavevector-frequency representation,

$$-i\omega\rho_1(\mathbf{k}, \omega) + \rho_0\mathbf{k} \cdot \mathbf{v}(\mathbf{k}, \omega) = 0 \tag{B4a}$$

$$-i\omega\epsilon(\mathbf{k}, \omega) = -\frac{k^2\kappa}{\rho_0} [2a(k)\epsilon_1(\mathbf{k}, \omega) + b(k)\rho_1(\mathbf{k}, \omega)] \tag{B4b}$$

$$-i\omega\mathbf{v}(\mathbf{k}, \omega) + i\mathbf{k} [2c(k)\rho_1(\mathbf{k}, \omega) + b(k)\epsilon_1(\mathbf{k}, \omega)] = -\frac{\eta_1}{\rho_0} k^2 \mathbf{v}(\mathbf{k}, \omega) + \mathbf{k} \cdot \frac{\eta_1}{3} + \frac{\eta_2}{1} \frac{\mathbf{k} \cdot \mathbf{v}(\mathbf{k}, \omega)}{\rho_0}. \tag{B4c}$$

This is the equation satisfied by a viscously-damped, adiabatic sound wave. If we replace w by the undamped solution to Eq. (137), the relationship in (B7) is replaced by

$$\frac{2k^2\kappa a(k)}{\rho_0^2} \ll \sqrt{2c(k)\rho_0}k \equiv C_s k, \quad (\text{B9})$$

where C_s is the velocity of an adiabatic acoustic wave. This relation is satisfied at sufficiently small wavevectors, or sufficiently long wavelengths. The second regime is defined by the converse of the relationship above, i. e.

$$w \ll \frac{2k^2\kappa a(k)}{\rho_0^2} \quad (\text{B10})$$

Here the equation is, asymptotically,

$$\omega^2 = i\omega \frac{\frac{4}{3}\eta_1 + \eta_2}{\rho_0} k^2 - 2c\rho_0 k^2 \left[1 - \frac{b(k)^2}{4a(k)c(k)} \right] = O. \quad (\text{B11})$$

Now, the velocity is that of an isothermal sound wave. Replacing w by the solution to the undamped equation, we arrive at the alternate form of Eq. (1111)

$$\frac{2k^2\kappa a(k)}{\rho_0^2} > > \frac{b(k)^2}{2c(k)\rho_0} \left[1 - \frac{4a(k)c(k)}{b(k)^2} \right] k \equiv c_T k. \quad (\text{B12})$$

Here c_T is the velocity of an isothermal acoustic mode. This relation will hold when the wavevector is sufficiently large, or the wavelength is sufficiently small.

To find the final root of the global dispersion relation (B6), set $\omega = i\zeta$. The resulting equation is a cubic with real, positive coefficients. There is one real root, and that real root must be negative. If we anticipate that the ζ that solves the equation is of order k^2 , for small k , then the equation satisfied by ζ reduces to

$$\zeta = \frac{2a(k)k^2}{\rho_0^2} \left[1 - \frac{b(k)^2}{4a(k)c(k)} \right] = O(k^4). \quad (\text{B13})$$

This is the dispersion relation for thermal conduction.

APPENDIX C: EFFECTIVE HAMILTONIAN IN THE CASE OF TWO SCALAR FIELDS

Because there are two fluctuating fields to take into account in the calculation of g-jitter effects, the “bare” effective Hamiltonian is somewhat more complicated than in the case of

the scalar (i.e. single component order parameter) ϕ^4 model. In this Appendix we review the features, particularly the critical behavior, of a model for simple gas-liquid critical behavior that incorporates the effects of fluctuations in both the mass density and the energy density.

The most general case of a theory with two fluctuating scalar fields, one of which becomes critical at a temperature T_0 , has the following Ginzburg-Landau-Wilson expansion in the immediate vicinity of the critical point:

$$H[x(\mathbf{q}), y(\mathbf{q})] = \sum_{\mathbf{q}} r(q)x(\mathbf{q})x(-\mathbf{q}) + \frac{1}{N}u \sum_{\mathbf{q}_1+\dots+\mathbf{q}_4=0} x(\mathbf{q}_1)\dots x(\mathbf{q}_4) \\ + \frac{1}{\sqrt{N}}v \sum_{\mathbf{q}_1+\dots+\mathbf{q}_3=0} x(\mathbf{q}_1)y(\mathbf{q}_2)y(\mathbf{q}_3) + \sum_{\mathbf{q}} Ay(\mathbf{q})y(-\mathbf{q}). \quad (\text{c1})$$

All neglected terms are higher order in the fluctuating fields $x(\mathbf{q})$ and $y(\mathbf{q})$, and are irrelevant in the Renormalization Group sense. In the vicinity of the critical temperature, the “bare” quadratic coefficient $r(q)$ goes to zero while A is a nonzero positive constant.

Fluctuations in the critical field $x(\mathbf{q})$ will renormalize the coefficients $r(q)$, u , v and A . Because the quadratic terms influence the slow dynamics most strongly we concentrate on $r(q)$ and A . The ultimate form of $r(q)$ is well-known. Asymptotically

$$r(q) \rightarrow Q^{2-\eta} f((T - T_c)Q^{-1/\nu}, q/Q), \quad (\text{C2})$$

where ν is the correlation length exponent ($\propto (T - T_c)^{-\nu}$)—and Q is an inverse length scale, determined either by the correlation length (i.e. $Q \propto \xi^{-1}$) or by the internal wave-vector q ($Q \propto q$). This is just standard correlation function scaling.

Fluctuations in $x(\mathbf{q})$ act on the quadratic term $\sum_{\mathbf{q}} Ay(\mathbf{q})y(-\mathbf{q})$ through the “correlation bubble” $\langle C(\mathbf{q}) C(-\mathbf{q}) \rangle$, where

$$c(\mathbf{q}) = \frac{1}{\sqrt{N}} \sum_{\mathbf{q}_1} x(\mathbf{q} + \mathbf{q}_1)x(\mathbf{q}_1). \quad (\text{C3})$$

Because this bubble has the form of an energy-energy correlation function—in the language of the Ising spin model—straightforward scaling considerations yield for the renormalized A

$$A = Q^{2/\nu-d} g((T - T_c)Q^{-1/\nu}, q/Q), \quad (\text{C4})$$

with Q again an inverse length scale. This scaling form holds if the critical exponent for the specific heat at constant volume, $\alpha = 2 - d\nu$ is greater than zero, as it is in the case of the simple gas-liquid critical point. The rescaling of A is discussed in more detail in the next Appendix.

Now, the two fields $x(\mathbf{q})$ and $y(\mathbf{q})$ are linear combinations of the energy density $\epsilon(\mathbf{q})$ and the mass density $\rho(\mathbf{q})$. Specifically, we assume

$$y(\mathbf{q}) = \alpha\epsilon(\mathbf{q}) + \beta\rho(\mathbf{q}) \quad (\text{C5a})$$

$$x(\mathbf{q}) = \gamma\epsilon(\mathbf{q}) + \delta\rho(\mathbf{q}). \quad (\text{C5b})$$

Substituting into Eq. (C1), we obtain the following free energy in p and ϵ , to quadratic order in the two densities:

$$F[\epsilon, \rho] = \sum_{\mathbf{q}} [a(q)\epsilon(\mathbf{q})\epsilon(-\mathbf{q}) + b(q)\epsilon(\mathbf{q})\rho(-\mathbf{q}) + c(q)\rho(\mathbf{q})\rho(-\mathbf{q})], \quad (\text{C6})$$

where

$$a(q) = r(q)\alpha^2 + A\gamma^2 \quad (\text{C7a})$$

$$b(q) = 2r(q)\alpha\beta + 2A\gamma\delta \quad (\text{C7b})$$

$$c(q) = r(q)\beta^2 + A\delta^2. \quad (\text{C7c})$$

The coefficients $a(q)$, $b(q)$, and $c(q)$ are dominated by the contributions of A in the immediate vicinity of the critical point, as the approach to zero of A is much gentler than that of $r(q)$. However, the sound velocity $C_s = 1/\sqrt{\beta_s \rho_c}$ vanishes as $t^{\alpha/2}$.

The behavior of the combination $a(q) - b(q)^2/4c(q)$ is another matter entirely. Using Eqs. (C7):

$$\begin{aligned} a - \frac{b^2}{4c} &= r\alpha^2 + A\gamma^2 - \frac{r^2\alpha^2\beta^2 + A^2\gamma^2\delta^2 + 2rA\alpha\beta\gamma\delta}{r\beta^2 + A\delta^2} \\ &= r \left[\alpha - \frac{\beta\gamma}{\delta} \right] + O \left(\frac{r^2}{A} \right). \end{aligned} \quad (\text{C8})$$

This combination scales as $r(q)$.

APPENDIX D: RENORMALIZATION OF THE COEFFICIENT A

In This Appendix, we fill in the details of the renormalization of the coefficient A in the Ginzburg-Landau equation, Eq. (C1). We start by introducing a field, $h(\mathbf{q})$, conjugate to the non-critical field $x(\mathbf{q})$. The portion of the Boltzmann factor the exponent of which is linear and quadratic in $x(\mathbf{q})$ is

$$\exp \left(- \sum_{\mathbf{q}} A x(\mathbf{q}) x(-\mathbf{q}) - v \frac{1}{\sqrt{N}} \sum_{\mathbf{q}_1 + \dots + \mathbf{q}_3 = 0} x(\mathbf{q}_1) y(\mathbf{q}_2) y(\mathbf{q}_3) + \sum_{\mathbf{q}} h(\mathbf{q}) x(-\mathbf{q}) \right), \quad (\text{D1})$$

Integrating over $x(\mathbf{q})$, we obtain the following contribution to the Boltzmann factor, where prefactors to the exponential have been neglected

$$\exp \left(- \sum_{\mathbf{q}} \frac{h(\mathbf{q}) h(-\mathbf{q})}{4A} + \frac{iv}{2A} \sum_{\mathbf{q}_1 + \dots + \mathbf{q}_3 = 0} h(\mathbf{q}_1) y(\mathbf{q}_2) y(\mathbf{q}_3) \right). \quad (\text{D2})$$

The second term in the above exponent represents an energy-like coupling to the $y(\mathbf{q})$'s. Integrating out those variables, we are left with the following quadratic term in the $h(\mathbf{q})$'s

$$- \frac{h(\mathbf{q}) h(-\mathbf{q})}{4A^2} v^2 Q^{d-2/\nu}, \quad (\text{D3})$$

where the quantity Q is an infrared momentum cutoff. There is, then, a gaussian contribution to the Boltzmann factor of the form

$$\exp \left(- \frac{h(\mathbf{q}) h(-\mathbf{q})}{4A} - \frac{h(\mathbf{q}) h(-\mathbf{q})}{4A^2} v^2 Q^{d-2/\nu} \right). \quad (\text{D4})$$

Finally, we re-introduce the variable $x(\mathbf{q})$ by multiplying the Boltzmann factor by $\exp \left(-i \sum_{\mathbf{q}} h(\mathbf{q}) x(-\mathbf{q}) \right)$ and integrating over $h(\mathbf{q})$. The result is the gaussian form

$$\exp \left(- \frac{A x(\mathbf{q}) x(-\mathbf{q})}{1 + v^2 Q^{d-2/\nu} / A} \right) \quad (\text{D5})$$

Now, if the critical exponent for the specific heat at constant volume, $\alpha = 2 - d\nu$ is greater than zero, then as $Q \rightarrow 0$ the renormalized coefficient A vanishes as $Q^{2/\nu-d}$, while A renormalizes to a *non-zero* value if $\alpha < 0$.

REFERENCES

- [1] M. Coleman and J. A. Lipa, *Phys. Rev. Lett.* **74**, 286 (1995)
- [2] M. R. Moldover, J. V. Sengers, R. W. Gammon and R. J. Hocken, *Rev. Mod. Phys.* **51**, 79 (1979)
- [3] Uniaxial ferromagnet in a nonuniform magnetic field.
- [4] A. W. Porter *Thermodynamics* (John Wiley & Sons, New York 1960), p. 30;
- [5] E. Ising, *Z. Phys.* **31**, 253 (1925).
- [6] See Volume VI of *Phase Transitions and Critical Phenomena*, C. Domb and M. S. Green, eds. (Academic Press, New York, 1976?).
- [7] K. Binder and D.W. Heermann, *Monte Carlo simulation in statistical physics : an introduction* (Springer-Verlag, New York, 1988)
- [8] C. Domb in Volume VI of *Phase Transitions and Critical Phenomena*, C. Domb and M. S. Green, eds. (Academic Press, New York, 1976?).
- [9] J. Rudnick and M. Barmatz in *Proceedings of the NASA/JPL 1994 Microgravity Low Temperature Workshop* JPLD-1 1775
- [10] R. A. Ferrell, *Ann. Physik* **2**, 26 (1993).
- [11] I. Hahn and M. Barmatz in *Proceedings of the NASA/JPL 1994 Microgravity Low Temperature Workshop* JPLD-1 1775
- [12] See, for instance *Acceleration Characterization and Analysis Report (ACAP): Early Summary of Mission Acceleration Experiments from STS-40* Gary L. Martin, Program Manager (NASA report).
- [13] E. D. Siggia, B. I. Halperin and P. C. Hohenberg, *Phys. Rev.* **13**, 2110 (1976).
- [14] P. C. Hohenberg and B. I. Halperin, *Rev. Mod. Phys.* **49**, 435 (1977).

- [15] H.E. Stanley, *introduction to Phase Transitions and Critical Phenomena* (Oxford University Press, New York, 1971).
- [16] L. P. Kadanoff and J. Swift, Phys. rev. 16689 (1968).
- [17] K. Kawasaki, Ann. Phys. (N. Y.) 61,1 (1970).
- [18] J. Wilks *The Properties of Liquid and Solid Helium* (Clarendon Press, Oxford, 1967)
- [19] C. E. Pittman, L. 11. Cohen and H. Meyer, J. Low Temp. Phys. 67, 237 (1987).
- [20]** C. C. Agosta, S. Wang, L. 11. Cohen and H. Meyer, J. Low Temp. Phys. 67,237 (1987).
- [21] B. Wallace and H. Meyer, Phys. Rev A 21563 (1970).
- [22] D.B. Roe and H. Meyer, J. Low Temp. Phys. 30,91 (1978)
- [23] G. R. Brown and H. Meyer, Phys. Rev. A 6,364 (1972).

FIGURES

FIG. 1. Some graphical elements of the Feynman Diagrams for critical dynamics. a : The heat diffusion propagator; b: The transverse velocity field propagator; c: The “parametric” effect of random linear accelerations on the transverse velocity field; d: The “parametric” effect of random rotations on the transverse velocity field

FIG. 2. One-loop correction to the thermal conductivity. The three-point vertices in the diagram are generated by the convective term in the heat transport equation (Eq.(A8b)) and the term $\frac{1}{\rho} \frac{\delta F}{\delta \epsilon} \nabla \epsilon$ in Eq.(A8c).

FIG. 3. Insertion on the transverse velocity propagator line generated by random rotations

TABLES

TABLE I. Definitions of the quantities appearing in the text, and the scaling behavior of critical thermodynamic functions and transport coefficients. The quantity t is the reduced temperature, $t = (T - T_c)/T_c$.

Quantity	Definition	Dominant scaling behavior (if any)
T_c	Critical temperature	
ρ_c	Critical mass density	
ξ	Correlation length	$\propto t^{-\nu}$ ^a
$c_P = T \left(\frac{\partial S}{\partial T} \right)_P$	Specific heat at constant pressure	$\propto t^{-\gamma}$ ^a
$c_V = T \left(\frac{\partial S}{\partial T} \right)_V$	Specific heat at constant volume	$\propto t^{-\alpha}$ ^a
$\beta_T = -\frac{1}{V} \left(\frac{\partial V}{\partial P} \right)_T$	Isothermal compressibility	$\propto t^{-\gamma}$ ^a
$\beta_S = -\frac{1}{V} \left(\frac{\partial V}{\partial P} \right)_S$	Isentropic compressibility	$\propto t^{-\gamma}$ ^a
κ	Thermal conductivity	$\propto t^{-\nu x_\lambda}$ ^b
η_1	Shear viscosity	$\propto t^{-\nu x_\eta}$ ^b

^aref. [15]

^brefs. [16,17,13,14]

TABLE II. Relations between various exponents. d is the spatial dimensionality

$\alpha = 2 - d\nu$ ^a
$\gamma = \nu(2 - \eta)$ ^a
$x_\lambda + x_\eta = 4 - d + \eta$ ^b

^aref. what?

^brefs. [16,17,13,14]

TABLEIII. Numerical values of some of the quantities that are used in the calculations relevant to ${}^3\text{He}$. uncertainties are not recorded here but may be found in the cited references.

Quantity	Definition	Value
u	Specific heat exponent	0.63^{a}
η	Anomalous dimension exponent	0.0002^{a}
x_λ	Thermal conductivity exponent	0.916^{b}
ρ_c	Critical density	$0.042 \text{ g/cm}^3^{\text{c}}$
$k_B T_c$	Critical temperature (in cgs)	$4.58 \times 10^{-16} \text{ g cm}^2/\text{sec}^2^{\text{c}}$
$D_T = \frac{\kappa \rho_c}{T_c c_P}$	Thermal diffusivity	$1.96 \times 10^{-4} t^{0.75} \text{ cm}^2/\text{sec}^{\text{d}}$
η_s/ρ_c	Shear viscosity	$3.99 \times 10^{-4} t^{-0.034} \text{ cm}^2/\text{sec}^{\text{e}}$
β_T	isothermal compressibility	$1.86 \times 10^{-7} t^{-1.18} \text{ cm sec}^2/\text{g}^{\text{f}}$
C_s	Velocity of sound (at low frequency)	$3.2 \times 10^4 t^{0.057} \text{ cm/sec}^{\text{g}}$
ξ	Correlation length	$2.56 \times 10^{-8} t^{-0.63} \text{ cm}^{\text{g}}$
c_P	specific heat at constant pressure	$2.53 \times 10^7 t^{-1.18} \text{ ergs/g}^\circ \text{ K}^{\text{h}}$

^aref.1

^brefs. [13,14]

^cref. [18]

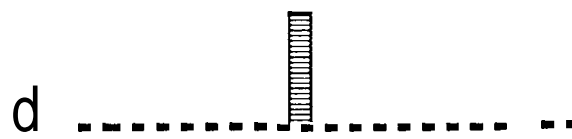
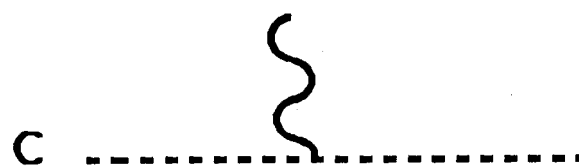
^dref. [?]

^eref. [20]

^fref. [21]

^gref. [22]

^href. [23]



The figure consists of four sub-diagrams labeled a, b, c, and d, arranged in a 2x2 grid. Each diagram shows a horizontal line with various features:

- a**: A horizontal dashed line.
- b**: A horizontal solid line.
- c**: A horizontal dashed line with a wavy vertical line segment extending upwards from its center.
- d**: A horizontal dashed line with a vertical hatched line segment extending upwards from its center.

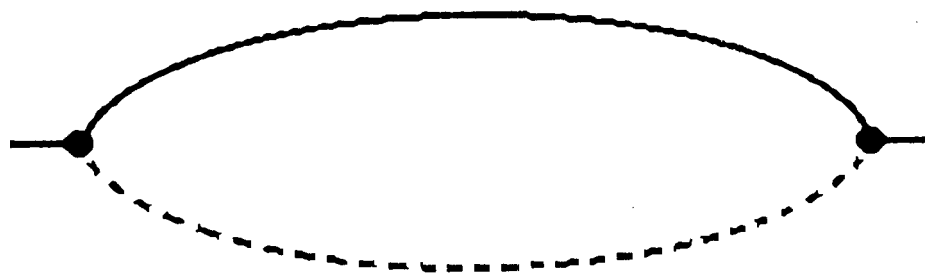


Fig. 2



Fig. 3